DOI: 10.1002/ejic.200700772

ortho-Directed Metathetical Fluoride/Amide Exchange in (Pentafluorophenyl)-amides[‡]

Pavel L. Shutov,[a] Sergey S. Karlov,*[b] Klaus Harms,[a] Maxim V. Zabalov,[b] Jörg Sundermeyer,*[a] Jörg Lorberth,[a] and Galina S. Zaitseva[b]

Keywords: Fluorinated ligands / Amides / Nucleophilic substitution / Density functional calculations

The indium tris(amide)s $[(Et_2N)_{3-n}In\{N(C_6F_5)(2\text{-}C_5H_4N)\}_n]$ [*n* = 1 (**15**), 2 (**16**) or 3 (**9**)] have been prepared by treatment of $[In(NEt_2)_3]_2$ (**3**) with a stoichiometric amount of $(2\text{-}C_5H_4N)(C_6F_5)NH$ (**1**). The analogous reaction of $Bi(NMe_2)_3$ (**2**) with 3 equiv. of amine **1** and the treatment of $BiCl_3$ (**5**) with a stoichiometric amount of $(2\text{-}C_5H_4N)(C_6F_5)NLi$ (**4**) both lead to $[Bi\{N(C_6F_5)(2\text{-}C_5H_4N)\}_3]$ (**10**). In contrast, only the difluoride **11** or the monofluoride **12**, which are the products of intramolecular *ortho*-directed exchange of NMe_2 and F substituents, are obtained from the reaction of **2** with 1 or 2 equiv. of **1**, respectively. The reaction between $Me_3Sb(Hal)_2$ [Hal = Br (**7**) Cl, (**8**)] and 1 or 2 equiv. of lithium salt **4** gives the corresponding stable monoamides $[Me_3(Hal)Sb\{N(C_6F_5)(2\text{-}C_5H_4N)\}]$ [Hal = Br (**17**), Cl (**18**)] or bis(amide) $[Me_3Sb\{N(C_6F_5)(2\text{-}C_5H_4N)\}_2]$ (**19**), respectively. The structure of **9** has been confirmed by an X-ray structure analysis, and density functional calculations data have been used to explain the possible reaction pathway of the *ortho*-directed metathetical fluoride/amide exchange.

Introduction

There has been a strong interest in activation of the C–F bond in polyfluoro organic compounds during the past several decades due to the possible utilization of these activation processes in organic synthesis.[2,3] A variety of methods for activating C–F bonds with transition metal centers have been published recently, and several examples based on early, middle, or late transition metal compounds have been used for the replacement of an F atom in polyfluoroaryl moieties, mostly by oxidative addition reactions.[4–11] Nucleophilic substitution reactions of an aryl carbon–fluorine bond assisted by main group element compounds (alkali and alkaline earth metals or silicon derivatives) have also been widely investigated.[4,5,12,13] However, to the best of our knowledge, most of the mechanistically studied examples have been ascribed to *intermolecular* processes. Assumptions about *intramolecular* pathways have been made exclusively for *ortho*-directed fluorine atom substitution for C_6F_5X species (X is a *ortho*-directing donor functionality) in reactions with Li or Mg reagents such as ArLi, RMg(Hal), ArMg(Hal) or ArN(R)Mg(Hal).[13,14]

Recently, we reported the reaction of $Sb(NEt_2)_3$ with $C_6F_5(2\text{-}C_5H_4N)NH$ (**1**), which leads to the antimony tris(amide)s $[(Et_2N)_2Sb\{N(C_6F_5)(2\text{-}C_5H_4N)\}]$, $[(Et_2N)Sb\{N(C_6F_5)(2\text{-}C_5H_4N)\}_2]$, and $[Sb\{N(C_6F_5)(2\text{-}C_5H_4N)\}_3]$ with one, two, or three pentafluoro(2-pyridyl)anilido groups.[1] Trivalent antimony compounds containing one or two NEt_2 groups are unexpectedly unstable, and they rearrange to give the bis(amido)antimony fluorides $[SbF\{N(C_6F_5)(2\text{-}C_5H_4N)\}_2]$ and $[(Et_2N)SbF\{N(C_6F_5)(2\text{-}C_5H_4N)\}]$, in almost quantitative yield at room temperature within 21 d.[1] To the best of our knowledge no such intramolecular rearrangements have been reported previously except in a paper by Schrock et al., where a similar nucleophilic substitution product is reported in low yield in the reaction of $Mo(NMe_2)_4$ with $(C_6F_5NHCH_2CH_2)_2NMe$.[15] In order to gain further insight into the fluoride/amide metathesis assisted by antimony, and to expand the scope of this reaction, we report herein our investigation of the analogous transamination reactions of $Bi(NMe_2)_3$ (**2**) and $[In(NEt_2)_3]_2$ (**3**) with $C_6F_5NH(2\text{-}C_5H_4N)$ (**1**). The reactions of the lithium salt of amine **1**, namely $C_6F_5NLi(2\text{-}C_5H_4N)$ (**4**), with $BiCl_3$ (**5**), $InCl_3$ (**6**), Me_3SbBr_2 (**7**), and Me_3SbCl_2 (**8**) are also reported. The structure of the novel monomeric indium tris(amide) $[In\{N(C_6F_5)(2\text{-}C_5H_4N)\}_3]$ (**9**) is confirmed by X-ray crystallography, and density functional calculations are used to distinguish possible rearrangement pathways.

[‡] The Case of Bismuth and Indium, II. Part I: Ref.[1]

[a] Fachbereich Chemie, Philipps-Universität Marburg, Hans-Meerwein-Strasse, 35032 Marburg/Lahn, Germany
Fax: +49-6421-28-28917
E-mail: jsu@chemie.uni-marburg.de
[b] Chemistry Department Moscow State University, B-234 Leninskie Gory, 119899 Moscow, Russia
Fax: +7-95-932-8846
E-mail: sergej@org.chem.msu.ru

Supporting information for this article is available on the WWW under http://www.eurjic.org or from the author.

Results and Discussion

Synthesis

Ligand **1** was first prepared by treating 2-bromopyridine with (pentafluorophenyl)amine,[16] although recently Ashenhurst et al. have used the approach of Koppang for the synthesis of **1**,[17] which involves the treatment of C_6F_6 with an equimolar mixture of (2-pyridylamido)lithium and $LiNH_2$.[18] We also used this reaction to prepare amine **1**, although we modified the method according to Equation (1). The twofold excess of lithiated 2-pyridylamine per mol of C_6F_6 is essential as product **1** is acidic enough to quench the nucleophile.

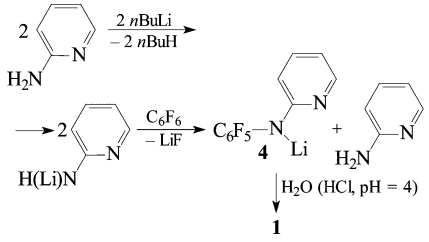

(1)

Treatment of $Bi(NMe_2)_3$ (**2**) with 3 equiv. of amine **1** in toluene and the reaction of lithium amide **4** with $BiCl_3$ (**5**) both afforded tris(amide) **2** in good yield [Equation (2)].

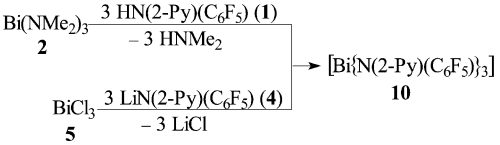

(2)

Treatment of $Bi(NMe_2)_3$ (**2**) with 1 or 2 equiv. of amine **1** led to difluoride **11** and monofluoride **12**, respectively, as products of a rearrangement reaction (Scheme 1). The instability of the plausible intermediates $[(NMe_2)_{3-n}Bi\{N(C_6F_5)(2\text{-}C_5H_4N)\}_n]$ is in sharp contrast to the corresponding antimony compounds, which only rearrange after extended reaction times.[1] Moreover, traces of both **11** and **12** were detected by NMR spectroscopy during the reaction of **2** with 3 equiv. of **1**. Thus, intramolecular nucleophilic substitution at a C_6F_5 moiety assisted by bismuth proceeds much faster than that for antimony derivatives. Hydrolysis of **11** and **12** led to the tris(amine)s **13** and **14**, which are difficult to synthesize by other methods.

In contrast to the reaction patterns of Sb and Bi compounds, the transamination of In amide **3** with 1, 2, and 3 equiv. of **1** selectively led to the corresponding tris(amide)s **15**, **16**, and **9**, respectively. No similar rearrangement processes were found in these studies [Equation (3)].

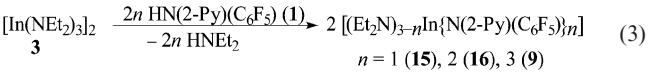

(3)

The tendency to rearrange is higher for compounds with a large covalent radius, low coordination number, and highly polar M–N bonds. We assume that this is probably more due to kinetic than to thermodynamic reasons. If the covalent character in M–N bonding is increased, for example by increasing the formal oxidation state of the central atom, the compounds become more inert with respect to rearrangement reactions: we observed that reaction of 1 or 2 equiv. of lithium amide **4** with $(Hal)_2SbMe_3$ (**7** and **8**) led to the expected unrearranged monoamides **17** and **18** or diamide **19** [Equation (4)]. While Sb^{III} amides tend to rearrange, Sb^{V} amides are inert with respect to this fluoride/amide exchange under ambient conditions.

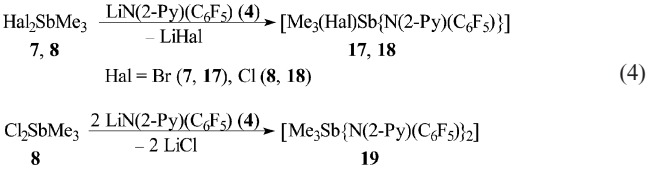

(4)

NMR Spectroscopic Study

The ^1H, ^{13}C, and ^{19}F NMR spectra of all compounds are consistent with a κ^2-*N*,*N*′-bonding mode of the 2-pyridylamido ligands. The solution spectra of bismuth fluo-

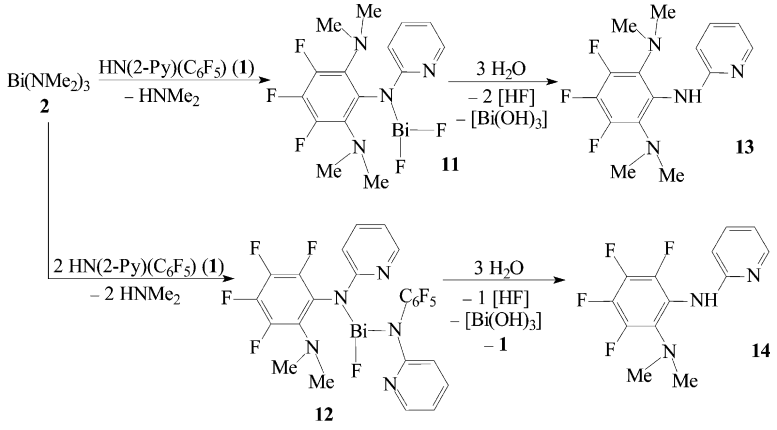

Scheme 1.

rides **11** and **12** are very similar to their previously characterized Sb analogs.[1] As already observed, the presence of one or two NMe_2 groups adjacent to the *ipso*-C atom of the aromatic rings inhibits the rotation of these moieties about the N–C_{ipso} bond. N-coordination in a chelate ring leads to the appearance of two signals for the NMe_2 group in the ^1H NMR spectra of **11** and **12**. In accordance with these data, we assume that indium compounds **9**, **15**, and **16** are monomeric chelate complexes in C_6D_6 solutions.

It should be noted that two different configurations (*fac* and *mer*) are possible for indium and bismuth tris(amide)s **9** and **10**. Ashenhurst et al. found recently that the closely related Al derivative $[Al\{N(C_6F_5)(2\text{-}C_5H_4N)\}_3]$ undergoes a dynamic *fac*/*mer* isomerization in $CDCl_3$ solutions at 25 °C.[18] The broadening of the signals in the ^1H and ^{13}C NMR spectra of **9** and **10** indicates that a similar isomerization process probably takes place here as well. The ability of both **9** and **10** to isomerize in solution was confirmed by the very close values of total energy for both isomers (see Density Functional Calculations section below).

Molecular Structure of 9

The molecular structure of **9** is shown in Figures 1 and 2, and Table 1 summarizes selected geometrical parameters. Compound **9** possesses a monomeric structure in the solid state. The coordination sphere of the indium atom is a distorted InN_6 octahedron with three amido groups and three pyridyl nitrogen atoms in a *fac* arrangement similar to the structurally related complex $[Al\{N(C_6F_5)(2\text{-}C_5H_4N)\}_3]$.[18] The distortion from octahedral geometry appears to be induced by the steric constraints of the $C_6F_5N(2\text{-}C_5H_4N)$ ligand. Analysis of the Cambridge Structural Database (Version 5.28, November 2006)[19] reveals more than ten structures with a similar InN_6 structural fragment, most of which contain either pyrazolylborate or phthalocyanine ligands or have ionic structures such as $In(NCS)_6^{3-}$. Interestingly, the most closely related structure, that of $[In(N_3)_3\text{-}Py_3]$,[20] possesses a *mer* configuration. As expected, the covalent In–N_{amido} bonds in **9** [2.174(3)–2.202(2) Å] are shorter than the donor–acceptor In–N_{Py} bonds [2.259(2)–2.324(3) Å].

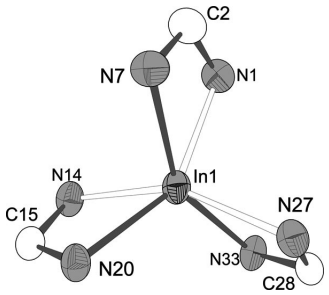

Figure 2. Thermal ellipsoid drawing of the indium coordination polyhedron in complex **9**.

Table 1. Selected bond lengths [Å] and angles [°] for complex **9** with estimated standard deviations in parentheses.

N1–In1	2.324(3)	N20–In1	2.202(3)
N7–In1	2.174(3)	N27–In1	2.259(2)
N14–In1	2.265(3)	N33–In1	2.190(3)
N7–In1–N33	147.9(1)	N20–In1–N14	59.75(8)
N7–In1–N20	97.3(1)	N27–In1–N14	153.64(9)
N33–In1–N20	112.7(1)	N7–In1–N1	58.8(1)
N7–In1–N27	103.98(9)	N33–In1–N1	95.4(1)
N33–In1–N27	59.92(9)	N20–In1–N1	149.61(9)
N20–In1–N27	102.20(8)	N27–In1–N1	101.83(9)
N7–In1–N14	97.7(1)	N14–In1–N1	102.16(9)
N33–In1–N14	106.94(9)		

No short contacts between In and the fluorine atoms of the C_6F_5 groups are found in the solid state. The shortest In···F contact in **9** of 3.585 Å (where F is an *ortho*-fluorine

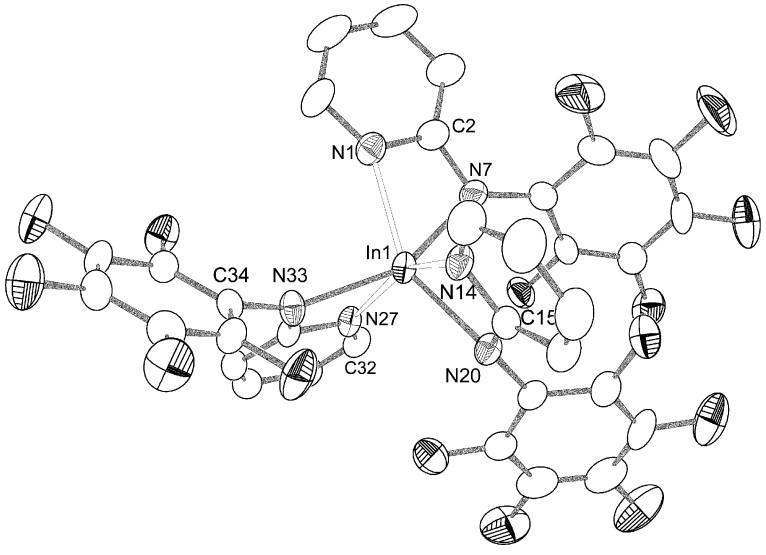

Figure 1. Thermal ellipsoid drawing of complex **9**. Hydrogen atoms and disordered toluene have been omitted for clarity. Displacement ellipsoids are drawn at the 50% probability level.

atom) is larger than the sum of the van der Waals radii of indium and fluorine (3.40 Å).[21]

Density Functional Study on Metal Complexes and Nucleophilic Substitution Reactions

To gain a better understanding of the driving force behind the *ortho*-directed metathetic fluoride/amide rearrangements we carried out density functional calculations at the PBE level of theory on a number of stable compounds and metastable intermediates on the reaction coordinate. The calculated structures and the reactions studied are presented in Scheme 2.

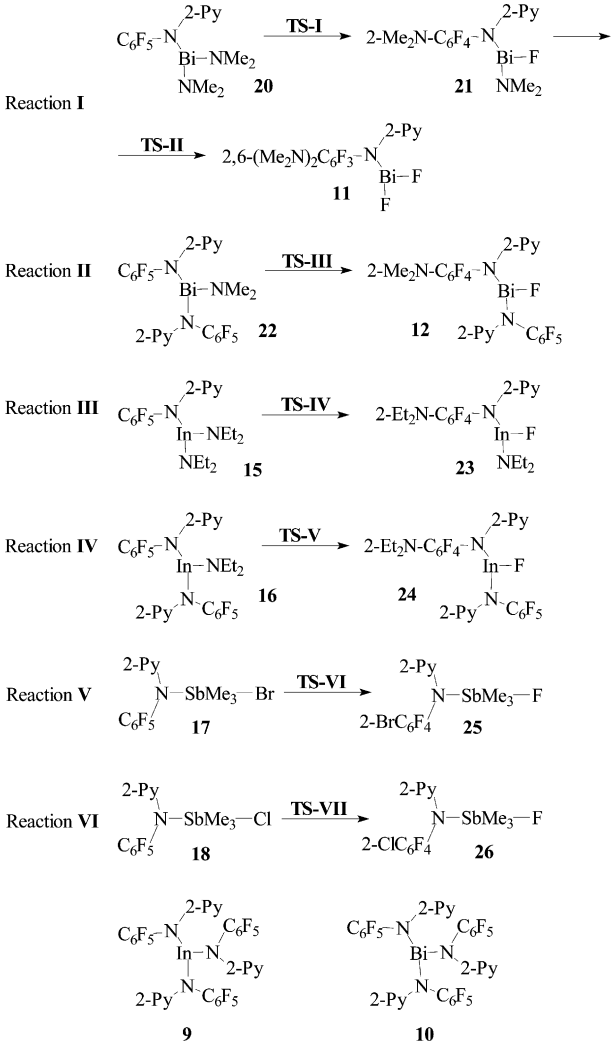

Scheme 2.

The compounds are likely to possess intramolecular contacts between the metal atom and the pyridine nitrogen atoms, therefore two different types of molecules were studied: derivatives containing additional intramolecular $N_{Py}\rightarrow M$ contacts (a) and derivatives without these contacts (b). In the cases where several additional $N_{Py}\rightarrow M$ contacts are possible, structures with the maximum number of contacts were calculated. The most important geometry parameters of species in series (a) are listed in Table 2; the calculated molecular structures of the compounds studied, the most important geometry parameters of these species, and the values of their total energies are listed in the Supporting Information. According to the results of the density functional calculations, the values of total energy for derivatives (a) with $N_{Py}\rightarrow M$ bonds are larger than those for the corresponding compounds (b) without these contacts for all species studied. The differences between the energy values for the starting materials lie within the range 7.03 (**20**) to 35.04 kcal mol^{-1} (**16**). The analogous values for the rearrangement products are 5.89 (**20**) to 41.27 kcal mol^{-1} (**16**).

It is of interest to note that the total energy of **9a**(*fac*) is practically identical to that of **9a**(*mer*): $\Delta E = E$[**9a**(*fac*)] – E[**9a**(*mer*)] = 1.16 kcal mol^{-1}; the same ΔE value was found for the Bi compound **10a**. This energy equivalence testifies to the possibility of *fac*/*mer* conformational exchange in solution for **9** and **10**, as proposed on the basis of the NMR spectroscopic data. The total energy values of **9a** and **10a**, which possess $N_{Py}\rightarrow M$ bonds, are also larger than those for **9b** and **10b**, respectively. These differences are 51.41 [**9**(*fac*)] and 52.49 kcal mol^{-1} [**9**(*mer*)], and 39.56 [**10**(*fac*)] and 35.31 kcal mol^{-1} [**10**(*mer*)]. We can therefore expect that all metal derivatives of the $C_6F_5N(2\text{-}C_5H_4N)$ ligand in question possess intramolecular coordination in solution [series (a)].

It should be noted that the calculated parameters of compound **9a**(*fac*) (In–N_{amido} 2.256 Å; In–N_{Py} 2.332–2.333 Å) are close to those found for the solid-state structure of **9** (see above). Consequently, we believe that the theoretical method used gives reasonable results for indium derivatives; the appropriateness of this method for Sb and Bi compounds was confirmed by us previously.[1,22]

Taking into consideration that no X-ray structure of prepared or proposed compounds is reported except for that of **9a**, the calculated geometrical data for the molecules studied [series (a), with $N_{Py}\rightarrow M$] are of particular interest. The primary coordination environment of the Bi atom in **11a**, **12a**, and **20a**–**22a** may be treated as a trigonal pyramid as the Bi–N_{Py} distances are smaller than the sum of the van der Waals radii of bismuth and nitrogen (3.94 Å).[21] Consequently, the Bi atom can be regarded as [3+1]-coordinate in **20a** and [3+2]-coordinate in **22a**. Analogous [3+2]-coordination is found in **11a** due to additional interaction of the Bi atom with one NMe_2 group. In contrast to **11a**, however, the Bi atom in **21a** should be regarded as [3+1]-coordinate because no interaction between the Bi atom and NMe_2 group is found in this compound. The Bi atom in **12a** possesses three additional contacts with nitrogen atoms (two N_{Py} and one NMe_2), which means that the distortion of the primary trigonal-pyramidal coordination environment of the bismuth atom is maximal. The starting compounds **20a**, **21a**, and **22a** also possess a short Bi–F contact (3.592, 3.378, and 3.431 Å, respectively).

The coordination polyhedron of the In atom in **15a** and **16a** is a distorted tetrahedron (two In–NEt_2 and one In–N_{amide} and In–N_{Py} bonds) and a distorted trigonal bipyramid (In–NEt_2 and two In–N_{amide} and In–N_{Py} bonds),

Table 2. Selected bond lengths [Å] for compounds **9a**–**12a**, **15a**–**18a**, **20a**–**26a**, and **TSIa**–**TSVIIa** (calculated data). X-ray data for **9** are given in square brackets.

Compound	M–N_{amide}	M–N(py)	M–NR_2	M–F[a]	M–Hal
9a(*fac*)	2.256, 2.256, 2.256, [2.174(3)], [2.190(3)], [2.202(3)]	2.332, 2.332, 2.332, [2.259(2)], [2.265(3)], [2.324(3)]	–	3.873 [3.585]	–
9a(*mer*)	2.261, 2.267, 2.276	2.318, 2.333, 2.299	–	3.571	–
10a(*fac*)	2.295, 2.397, 2.409	2.556, 2.558, 2.609	–	3.610	–
10a(*mer*)	2.319, 2.349, 2.363	2.590, 2.641, 2.735	–	3.660	–
20a	2.308	2.772	2.165, 2.190	3.592	–
TSIa	2.213	2.659	2.150, 2.396[b]	3.122,[c]	–
21a	2.276	2.680	2.146, 4.838[d]	2.077,[e] 3.378	–
TSIIa	2.215	2.578	2.330,[b] 5.058[d]	2.07,4[e] 2.767[c]	–
11a	2.243	2.502	2.551,[f] 5.019[d]	2.150,[e] 2.168[e]	–
22a	2.297, 2.299	2.701, 2.781	2.182	3.431	–
TSIIIa	2.262, 2.234	2.650, 2.766	2.356[b]	2.938[c]	–
12a	2.284, 2.406	2.483, 3.026	2.581[f]	2.165[e]	–
15	2.280	2.317	2.084, 2.092	3.524	–
IVa	2.198	2.355	2.080, 2.239[b]	2.437[c]	–
23a	2.224	2.276	2.109, 4.008[d]	2.014[e]	–
16	2.244, 2.250	2.336, 2.342	2.084	3.420	–
Va	2.175, 2.269	2.253, 2.424	2.245[b]	2.494[c]	–
24a	2.201, 2.315	2.303, 2.388	2.608[f]	2.035[e]	–
17a	2.275	2.363	–	3.721	2.707
VIa	2.199	3.122	–	2.260[c]	2.905[b]
25a	2.302	2.322	–	2.007	4.239[d]
18a	2.274	2.357	–	3.729	2.528
VIIa	2.192	3.203	–	2.280[c]	2.761[b]
26a	2.297	2.325	–	2.007	4.127[d]

[a] Shortest distance for the molecule. [b] Splitting bond. [c] Nascent bond. [d] No interaction. [e] Covalent bond. [f] Dative bond.

respectively. Compounds **15a** and **16a** also possess a short In–F contact (3.524 and 3.420 Å, respectively). These values are comparable with those found for bismuth derivatives (see above), although the smaller covalent and van der Waals radii of indium in comparison with those of bismuth should be noted.

The coordination polyhedron of the Sb atom in **17a** and **18a** is a distorted octahedron (three Sb–CH_3 and one Sb–N_{amide}, Sb–Hal, and Sb–N_{Py} bonds). These compounds do not possess any short Sb–F contacts (shortest distance: 3.721 and 3.729 Å, respectively).

As stated above, six reactions were studied during this work (Scheme 2). Analysis of the total energy values for the starting materials and products (Table 3) shows that the products are thermodynamically more favored in all the reactions studied. However, the experimental results show that reactions **I** and **II** proceed completely and compounds **20**–**22** are not detected in the reaction mixtures, while reactions **III**–**VI** do not take place. This means that kinetic factors are the key to understanding the origin of these processes. We therefore calculated the transition-state (TS) geometries of reactions **I**–**VI** for structures with (**TSIa**–**TSVIIa**) and without (**TSIb**–**TSVIIb**) N_{Py}→M interactions. The most important geometrical parameters of species in series (a) are listed in Table 2 and the molecular structures of the TSs studied, their atomic coordinates, and the total energy values are given as Supporting Information. Table 3 summarizes the relative energy values for the species studied, including the transition states **I**–**VII** (the activation barriers).

The computed barriers (Table 3) for the observed reactions **20a** → **21a**, **21a** → **11a**, and **22a** → **12a** in the gas phase are low (17.64–24.41 kcal mol^{-1}), while those for reactions **III**–**VI** are considerably higher (46.23–50.57 kcal mol^{-1}). The values found for the activation barrier in reactions **I** and **II** are very close to those previously found for the reaction [$(Et_2N)Sb\{N(C_6F_5)(2\text{-}C_5H_4N)\}_2$] → [$SbF\{N(C_6F_5)(2\text{-}C_5H_4N)\}_2$] (27.70 kcal mol^{-1}).[1] Similarly close values (21.8–41.2 kcal mol^{-1}, RB3LYP/DZVP level of theory) have been found for the activation barrier for the insertion of $Pd(PH_3)_2$ into the C–F bond of different fluoroarenes (FC_6H_3XY; X, Y = H, CN, NO_2).[23]

Table 3. ΔH [E_{total}(products) – E_{total}(reactants); kcal mol^{-1}] for reactions **I**–**VI** as well as activation barriers for these rearrangements (E_{act}; kcal mol^{-1}).

Reaction	I		II	III	IV	V	VI
	20a → 21a	**21a → 11a**	**22a → 12a**	**15a → 23a**	**16a → 24a**	**17a → 25a**	**18a → 26a**
ΔH	–28.72	–26.67	–22.86	–26.07	–31.87	–9.82	–9.36
E_{act}	17.64 (**TSIa**)	24.41 (**TSIIa**)	20.30 (**TSIIIa**)	46.77 (**TSIVa**)	50.57 (**TSVa**)	47.88 (**TSVIa**)	46.23 (**TSVIIa**)
	20b → 21b	**21b → 11b**	**22b → 12b**	**15b → 23b**	**16b → 24b**	**17b → 25b**	**18b → 26b**
ΔH	–29.85	–24.80	–23.36	–33.28	–25.64	–2.15	–1.05
E_{act}	24.64 (**TSIb**)	29.02 (**TSIIb**)	25.59 (**TSIIIb**)	16.17 (**TSIVb**)	31.00 (**TSVb**)	36.17 (**TSVIb**)	34.01 (**TSVIIb**)

The computed barriers for the system without N_{Py}→M bonds [series (b)] are different from those previously discussed for species which contain N_{Py}→M contacts [series (a)]. While the values for reactions **20b** → **21b**, **21b** → **11b**, **22b** → **12b**, **17b** → **25b**, and **18b** → **26b** are close to those found previously (see Table 3), the barriers for reactions of indium species **15b** → **23b** and **16b** → **24b** are dramatically lower than those for reactions **15a** → **23a** and **16a** → **24a**.

Some general trends should be noted with regard to the calculated transition state geometries [series (a)]. First of all, the species are characterized by a considerable shortening of the M–F contacts in comparison with those found in reactants **15a**–**18a** and **20a**–**22a**, while the splitting bond (M–N or Sb–Hal) becomes elongated. Some elongation of the M–N_{Py} distances in the TSs in comparison with those in the corresponding reactants should be mentioned, especially the significant alterations in **TSVIa** and **TSVIIa**.

A noticeable elongation of both C–C bonds (aromatic C_6F_5 ring) at the carbon atom involved in the rearrangement processes is also found for all TSs studied. The values of the nascent C–N bond lengths in **TS1a**–**TSVa** vary between 1.760 and 1.991 Å, while the corresponding covalent bonds in the products of reactions **I**–**IV** are 1.399–1.461 Å. Analogously, the values of the splitting C–F bond lengths in **TS1a**–**TSVa** vary between 1.482 and 1.565 Å, while the corresponding covalent bonds in the reactants of reactions **I**–**IV** are 1.348–1.356 Å. The F–C–N angles in **TS1a**–**TSVa** vary between 85.6 and 92.6°. The geometry of the transition states therefore allows us to define the proposed mechanism of the nucleophilic addition under study as a concerted oxidative addition.[11,24,25]

We believe that the main driving force behind the studied rearrangements is the formation of thermodynamically more favorable species. In the case of bismuth derivatives **20a**, **21a**, and **22a**, as well as the previously studied antimony compounds $[(Et_2N)_2Sb\{N(C_6F_5)(2\text{-}C_5H_4N)\}]$ and $[(Et_2N)Sb\{N(C_6F_5)(2\text{-}C_5H_4N)\}_2]$,[1] these interconversions proceed very easily as the weak N_{Py}→M contacts in these substances do not prevent M–F bond formation. In our opinion the rearrangement is likely to proceed through formation of a hypervalent fragment $C_{C_6F_5}$–F–Bi(Sb) with retention of the Bi(Sb)–NR_2 bond in **TS1a**–**TSIIIa**. Thus, the presence of additional electron density on the metal atom is necessary to decrease the activation barrier of the studied rearrangement.

In contrast, the indium derivatives **15** and **16** are stable and do not participate in any rearrangement processes due to the very strong N_{Py}→In interaction. The presence of this bond in indium derivatives increases the steric hindrance to the attack of the F atom at the In atom, although the indium center is more electron-deficient than in compounds without additional interactions. Both these factors prevent the rearrangement of **15** and **16** from occurring. This conclusion is confirmed by the decrease of the computational barrier found for **15b** → **23b** and **16b** → **24b** (compounds without N_{Py}→In contacts).

As regards reactions **V** and **VI**, we believe that the high barriers are caused by factors analogous to those previously mentioned for indium derivatives. The comparatively strong N_{Py}→Sb interaction along with the presence of five covalent bonds around the antimony atom in **17a** and **18a** prevent these Sb centers from participating in the supposed rearrangement. It should be noted, however, that the difference between the reactants and products in these reactions is not as large as in other reactions studied (Table 3).

Conclusions

In an extension of our studies on antimony(III) amides we have investigated the transamination of pentafluoro(2-pyridyl)aniline with dialkylamides of bismuth(III), antimony(V), and indium(III). The reaction between $Bi(NMe_2)_3$ (**2**) and $HN(2\text{-}C_5H_4N)(C_6F_5)$ (**1**) affords the expected tris(amide) **10**, whereas replacement of only one or two NMe_2 groups leads to the isolation of the unexpected bismuth fluorides **11** and **12** as a result of an F↔NMe_2 metathesis. In contrast, the treatment of $[In(NEt_2)_3]_2$ (**2**) with the same amine **1** leads to the corresponding stable monomeric tris(amide)s **9**, **15**, or **16**. No F↔NEt_2 rearrangement occurs for **15** and **16**. Furthermore, antimony(V) amides such as **17** and **18** tend to be more stable with respect to this rearrangement than the antimony(III) amides reported previously. These examples show that the tendency to undergo this rearrangement increases with an increase of the covalent radius and decreases with an increase of coordination number of the central atom. This rearrangement also requires a highly polar M–N bond, therefore increasing the covalent character of the compound (e.g. by a higher oxidation state) decreases the likelihood of this metathesis to occur. Density functional calculations on the activation barriers of the studied reactions have been found to be in agreement with the experimental results. The steric demand of the substituents at the central atom as well as its electron deficiency are the crucial factors that define the stability of these tris(amide)s to F↔NR_2 or conceivable F↔Hal rearrangements.

Experimental Section

General Remarks: All manipulations were performed under dry, oxygen-free argon using standard Schlenk techniques. All manipulations of Bi-containing compounds were carried out in brown glass equipment. Solvents were dried by standard methods and distilled prior to use. $Bi(NMe_2)_3$ (**2**),[26] $[In(NEt_2)_3]_2$ (**3**),[27] Me_3SbBr_2 (**7**),[28] and Me_3SbCl_2 (**8**)[29] were prepared according to the literature. C_6D_6 was obtained from Deutero GmbH and dried with sodium. ^1H, ^{13}C, and ^{19}F NMR spectra were recorded with Bruker ARX 200, AC 300, AMX 400, or DRX 500 spectrometers at 23 °C. Chemical shifts in the ^1H and ^{13}C NMR spectra are given in ppm relative to internal Me_4Si, and those in ^{19}F NMR experiments relative to $CFCl_3$ as an external standard. EI mass spectra were recorded with a Finnigan MAT CH7A device using electron impact ionization at 70 eV, and FD mass spectra were recorded with a Finnigan MAT 95S device; all assignments were made with reference to the most abundant isotopes. Elemental analyses were carried out by the Fachbereich Chemie of the Philipps University

Marburg (Heraeus-Rapid-Analyzer). The nonempirical generalized gradient approximation (GGA) for the exchange-correlation functional of Perdew et al. (PBE) was employed in this work.[30,31] All calculations were performed using the program PRIRODA developed by Laikov,[32] which implements an economical computational procedure. The one-electron wavefunctions were expanded in the extended TZ2P atomic basis sets of the contracted Gaussians {311/1} for H, {611111/411/11} for C, N, and F, {6111111111/611111/11} for Cl, {6111111111111/5111111111/51111} for Br, {711111111111111/611111111111/51111111} for In and Sb, and {24,24,24,24,24,24,24,24/22,22,22,22,22,22,22,22/15,15,15,15,15/9} for Bi. Full geometry optimization was performed by DFT-PBE methods for a number of structures followed by vibrational frequency calculation using analytical first and second derivatives. Each structure was characterized by a vibrational analysis. Each transition state has only one imaginary normal mode and equilibrium geometry states have only real normal modes. An IRC (intrinsic reaction coordinate) calculation was run starting from the transition state geometry in both directions and verified initial and final structures linked to the transition state. The present theoretical method has been used, and has given very useful results, in antimony and bismuth chemistry.[22]

Synthesis of (2-C_5H_5N)(C_6F_5)NH (1): *n*-Butyllithium (1.6 M in hexane, 325 mL, 0.52 mol) was added dropwise to a stirred solution of 2-aminopyridine (48.94 g, 0.52 mol) in thf (50 mL) at –78 °C. The reaction mixture was warmed to 25 °C and stirred at room temperature for 4 h, and then all volatiles were removed under reduced pressure; thf (300 mL) was added to the residue, and then a solution of C_6F_6 (48.36 g, 0.26 mol) in thf (60 mL) was added dropwise at –45 °C over about 1 h. The reaction mixture was warmed to room temperature and refluxed for a further 24 h. Dilute hydrochloric acid was then carefully added to the reaction mixture to pH = 4. The organic phase was washed twice with dilute hydrochloric acid (100 mL), and the combined aqueous phases were extracted with diethyl ether (2 × 100 mL). All organic phases were combined and dried with Na_2SO_4, and all volatiles were removed under reduced pressure. The residue was extracted with hot *n*-heptane, and crystallized crude **1** was purified by sublimation (50 °C/5×10^{-3} bar). Colorless crystals. Yield: 60.72 g (90%). EI-MS: *m*/*z* (%) = 260 (42) [M^+], 241 (100) [M^+ – F]. ^{1}H NMR (C_6D_6, 200.13 MHz): δ = 5.99 (m, 1 H), 6.36 (m, 1 H), 6.84 (br. s, 1 H, NH), 6.98 (m, 1 H), 8.07 (m, 1 H) ppm. ^{13}C NMR (C_6D_6, 50.32 MHz): δ = 108.45, 116.25, 137.78, 148.29, 155.29 (all carbon atoms of pyridyl groups) ppm; 4 signals for the carbon atoms of the C_6F_5 group were not observed in the spectrum. ^{19}F NMR (C_6D_6, 188.28 MHz): δ = –164.07 (t, 2 F), –161.80 (t, 1 F), –147.27 (d, 2 F) ppm.

Synthesis of 2-C_5H_5N(C_6F_5)NLi·thf (4·thf): *n*-Butyllithium (1.6 M in hexane, 22.50 mL, 36.00 mmol) was added dropwise to a stirred solution of **1** (9.33 g, 35.88 mmol) in thf (50 mL) at –78 °C. The reaction mixture was warmed to 25 °C and stirred at room temperature for 5 h, and then all volatiles were removed under reduced pressure to give a white solid. The crude product was washed with cold *n*-pentane (3 × 10 mL) and dried under reduced pressure. Yield: 11.03 g (91%). White solid. $C_{15}H_{12}F_5LiN_2O$ (338.20): calcd. C 53.27, H 3.58, N 8.28; found C 52.94, H 3.50, N 8.03. ^{1}H NMR (C_6D_6, 200.13 MHz): δ = 1.02–1.08 (m, 4 H, O-CH_2-CH_2), 3.20–3.26 (m, 4 H, O-CH_2), 6.16–6.27 (m, 2 H), 6.97–7.06 (m, 1 H), 7.84 (br. s, 1 H) ppm. ^{19}F NMR (C_6D_6, 188.28 MHz): δ = –173.52 (br. s, 1 F), –166.15 (t, F), –155.10 (br. s, 2 F) ppm. ^{19}F NMR (thf, 188.28 MHz): δ = –179.22 (t, 1 F), –170.14 (t, 2 F), –153.64 (d, 2 F) ppm.

Synthesis of [(2-C_5H_4N)(C_6F_5)N]$_3$Bi (10). Method a: A solution of amine **1** (0.76 g, 2.90 mmol) in toluene (10 mL) was added dropwise at 0 °C to a stirred solution of **2** (0.33 g, 0.97 mmol) in toluene (10 mL). The reaction mixture was stirred at room temperature for 12 h, and all volatiles were removed under reduced pressure. The residue was recrystallized from *n*-pentane (–30 °C) to give **10** as a yellow solid. Yield: 0.78 g (82%). **Method b:** A solution of **4**·thf (1.67 g, 4.96 mmol) in thf (15 mL) was added dropwise to a stirred suspension of $BiCl_3$ (0.52 g, 1.65 mmol) in thf (20 mL) at 0 °C. The reaction mixture was stirred for a further 12 h, and then all volatiles were removed under reduced pressure. *n*-Pentane (30 mL) was added to the residue, and insoluble substances were removed by filtration. The solution was reduced in volume to 20% of the original volume and stored at –30 °C to obtain **10** as a yellow solid. Yield: 1.20 g (74%). $C_{33}H_{12}BiF_{15}N_6$ (986.45): calcd. C 40.18, H 1.23, N 8.52; found C 39.79, H 1.43, N 8.03. EI-MS: *m*/*z* (%) = 727 (28) [M – N(C_5H_4N)(C_6F_5)]$^+$. ^{1}H NMR (C_6D_6, 200.13 MHz): δ = 5.58 (br. s, 3 H), 6.14 (br. s, 3 H), 6.93–7.02 (m, 3 H), 7.89 (br. s, 3 H) ppm. ^{13}C NMR (C_6D_6, 50.32 MHz): δ = 107.96, 112.33, 140.96, 144.17 ppm; 4 signals for the carbon atoms of the C_6F_5 group and 1 signal for a carbon atom of the pyridyl group were not observed in the spectrum. ^{19}F NMR (C_6D_6, 188.28 MHz): δ = –164.80 (br. s, 6 F), –162.64 (br. s, 3 F), –146.86 (d, 6 F) ppm.

Synthesis of 11: A solution of **1** (0.86 g, 3.3 mmol) in toluene (20 mL) was added dropwise to a stirred solution of **2** (1.15 g, 3.3 mmol) in toluene (15 mL) at –78 °C. The reaction mixture was stirred at room temperaturefor 24 h, and all volatiles were then removed under reduced pressure. The residue was recrystallized from *n*-pentane (–30 °C) to give **11** as a yellow solid. Yield: 1.21 g (66%). $C_{15}H_{16}BiF_5N_4$ (506.13): calcd. C 32.39, H 2.90, N 10.07; found C 31.27, H 2.98, N 9.20. FD-MS: *m*/*z* (%) = 519 (32) [M^+ – 2 F + H], 518 (20) [M^+ – 2 F]. ^{1}H NMR (C_6D_6, 200.13 MHz): δ = 2.37, 2.38 (2 s, 12 H, NMe_2) 5.70 (m, 1 H), 6.00 (m, 1 H), 6.98 (m, 1 H), 7.63 (m, 1 H) ppm. ^{19}F NMR (C_6D_6, 188.28 MHz): δ = –164.39 (br. s, 2 F, F_2Bi), –163.25 (t, 1 F), –149.50 (d, 2 F) ppm.

Synthesis of 12: A solution of **1** (0.62 g, 2.4 mmol) in toluene (10 mL) was added dropwise to a stirred solution of **2** (0.43 g, 1.3 mmol) in toluene (10 mL) at –78 °C. The reaction mixture was stirred at room temperature for 24 h, and then all volatiles were removed under reduced pressure. The residue was recrystallized from *n*-pentane (–30 °C) to give **12** as a yellow solid. Yield: 0.56 g (58%). $C_{24}H_{14}BiF_{10}N_5$ (771.37): calcd. C 37.37, H 1.83, N 9.08; found C 36.09, H 2.08, N 8.22. EI-MS: *m*/*z* (%) = 771 (1) [M^+]. FD-MS: *m*/*z* (%) = 772 (0.5) [M^+ + H], 771 (0.5) [M^+], 752 (2) [M^+ – F]. ^{1}H NMR (C_6D_6, 200.13 MHz): δ = 2.24, 2.25 (2 s, 6 H, Me), 5.83 (m, 1 H), 6.04 (m, 1 H), 6.10 (m, 1 H), 6.39 (m, 1 H), 7.02 (m, 1 H), 7.06 (m, 1 H), 7.57 (m, 1 H), 7.75 (m, 1 H) ppm. ^{19}F NMR (C_6D_6, 188.28 MHz): δ = –165.42 (t, 2 F), –165.26 (t, 1 F), –163.90 (t, 1 F), –162.96 (t, 1 F), –151.19 (d, 1 F), –146.70 (t, 2 F), –146.87 (br. s, 1 F, FBi), –142.78 (d, 1 F) ppm.

Synthesis of 13: Water (2 mL) was added dropwise to a stirred solution of **11** (0.72 g, 1.3 mmol) in toluene (10 mL), and the reaction mixture was stirred for 12 h. The organic phase was separated, dried with Na_2SO_4, and all volatiles were removed under reduced pressure. The residue was recrystallized from *n*-heptane (2 mL) to give **13** as a colorless solid. Yield: 0.26 g (65%). $C_{15}H_{17}F_3N_4$ (310.32): calcd. C 58.06, H 5.52, N 18.05; found C 57.63, H 4.09, N 17.64. EI-MS: *m*/*z* (%) = 310 (100) [M^+]. ^{1}H NMR (C_6D_6, 200.13 MHz): δ = 2.43, 2.44 (2s, 12 H, NMe_2), 6.12 (m, 1 H), 6.45 (m, 1 H), 7.06 (m, 1 H), 8.22 (m, 1 H) ppm. ^{13}C NMR (C_6D_6, 50.32 MHz): δ = 42.49, 42.59 (NMe_2), 109.17, 115.56, 136.52, 148.57, 155.44 ppm; 4 signals for the carbon atoms of C_6F_5 and 1

signal for a carbon atom of the pyridyl group were not observed in the spectrum. ^{19}F NMR (C_6D_6, 188.28 MHz): δ = –166.28 (t, 1 F), –150.42 (d, 2 F) ppm.

Synthesis of 14: Water (2 mL) was added dropwise to a stirred solution of **12** (0.43 g, 0.6 mmol) in toluene (10 mL), and the reaction mixture was stirred for 12 h. The organic phase was separated, dried with Na_2SO_4, and all volatiles were removed under reduced pressure. The residue was purified by chromatography (SiO_2; *n*-heptane/toluene (5:1), 30 mL) to give **14** as a colorless solid. Yield: 0.07 g (41%). $C_{13}H_{11}F_4N_3$ (285.24): calcd. C 54.74, H 3.89, N 14.73; found C 54.46, H 3.61, N 14.93. EI-MS: *m*/*z* (%) = 285 (100) [M^+]. ^1H NMR (C_6D_6, 200.13 MHz): δ = 2.25, 2.26 (2s, 6 H, NMe_2), 6.17 (m, 1 H), 6.38 (m, 1 H), 7.01 (m, 1 H), 8.16 (m, 1 H) ppm. ^{13}C NMR (C_6D_6, 50.32 MHz): δ = 43.00, 43.09 (NMe_2), 108.74, 116.23, 137.53, 148.60, 155.90 ppm. ^{19}F NMR (C_6D_6, 188.28 MHz): δ = –165.26 (t, 1 F), –162.93 (t, 1 F), –151.18 (d, 1 F), –142.78 (d, 1 F) ppm.

Synthesis of 15: A solution of amine **1** (0.30 g, 1.15 mmol) in toluene (10 mL) was added dropwise at –78 °C to a stirred solution of **3** (0.38 g, 0.58 mmol) in toluene (10 mL). The reaction mixture was stirred at room temperature for 12 h, and all volatiles were removed under reduced pressure. The residue was recrystallized from *n*-pentane (–30 °C) to give **15** as a yellow solid. Yield: 0.52 g (87%). $C_{19}H_{24}F_5InN_4$ (518.23): calcd. C 44.04, H 4.67, N 10.81; found C 43.57, H 4.41, N 10.04. EI-MS: *m*/*z* (%) = 374 (15) [M – 2 NEt_2]$^+$. ^1H NMR (C_6D_6, 200.13 MHz): δ = 0.97 (t, 12 H, CH_3), 2.48 (q, 8 H, NCH_2), 5.89–6.01 (m, 2 H), 6.78–6.86 (m, 1 H), 7.52–7.54 (m, 1 H) ppm. ^{13}C NMR (C_6D_6, 50.32 MHz): δ = 15.61 (CH_3), 44.18 (NCH_2), 107.96, 112.33, 140.96, 144.17 ppm; four signals for the carbon atoms of the C_6F_5 group and one signal for a carbon atom of the pyridyl group were not observed in the spectrum. ^{19}F NMR (C_6D_6, 188.28 MHz): δ = –165.63 (t, 1 F), –164.77 (t, 2 F), –149.89 (d, 2 F) ppm.

Synthesis of 16: The procedure was analogous to that used to synthesize **15**. Thus, treatment of a solution of **1** (1.46 g, 5.60 mmol) in toluene (10 mL) with a solution of **3** (1.46 g, 5.60 mmol) in toluene (10 mL) gave **16** as a light yellow solid. Yield: 1.46 g (74%). $C_{26}H_{18}F_{10}InN_5$ (705.26): calcd. C 44.28, H 2.57, N 9.93; found C 43.52, H 2.61, N 9.49. EI-MS: *m*/*z* (%) = 633 (76) [M – NEt_2]$^+$. ^1H NMR (C_6D_6, 300.13 MHz): δ = 0.68 (t, 6 H, CH_3), 3.29 (br. s, 4 H, NCH_2), 5.80–5.83 (m, 2 H), 6.09–6.13 (m, 2 H), 6.90–6.95 (m, 2 H), 7.47–7.49 (m, 2 H) ppm. ^{13}C NMR (C_6D_6, 75.47 MHz): δ = 12.10 (CH_3), 41.15 (NCH_2), 107.74, 110.81, 140.45, 144.27, 162.82 ppm; 4 signals for the carbon atoms of the C_6F_5 group were not observed in the spectrum. ^{19}F NMR (C_6D_6, 188.28 MHz): δ = –164.74 (t, 2 F), –163.37 (t, 4 F), –147.14 (d) ppm.

Synthesis of 9: A solution of amine **1** (1.87 g, 7.20 mmol) in toluene (10 mL) was added dropwise at room temperature to a stirred solution of **3** (0.80 g, 1.20 mmol) in toluene (10 mL). The reaction mixture was stirred for 12 h, and all volatiles were removed under reduced pressure. The residue was recrystallized from *n*-pentane (–30 °C) to give **9** as colorless crystals. Yield: 2.00 g (93%). $C_{33}H_{12}F_{15}InN_6$ (892.28): calcd. C 44.42, H 1.36, N 9.42; found C 44.20, H 1.27, N 8.86. EI-MS: *m*/*z* (%) = 892 (79) [M]$^+$, 633 (63) [M – N(C_5H_4N)(C_6F_5)]$^+$, 374 (10) [M – 2 N(C_5H_4N)(C_6F_5)]$^+$. ^1H NMR (C_6D_6, 300.13 MHz): δ = 5.92–5.95 (m, 3 H), 5.99–6.03 (m, 3 H), 6.80–6.86 (m, 3 H), 7.56–7.58 (m, 3 H) ppm. ^{13}C NMR (C_6D_6, 75.47 MHz): δ = 108.05, 112.69, 140.89, 144.41 ppm; 4 signals for the carbon atoms of the C_6F_5 group and 1 signal for a carbon atom of the pyridyl group were not observed in the spectrum. ^{19}F NMR (C_6D_6, 188.28 MHz): δ = –165.28 (br. s, 3 F), –164.66 (t, 6 F), –149.54 (br. s, 6 F) ppm.

Synthesis of 17: A solution of **4**·thf (1.64 g, 4.84 mmol) in thf (20 mL) was added dropwise at room temperature to a stirred solution of **7** (1.58 g, 4.84 mmol) in thf (15 mL). The reaction mixture was stirred at room temperature for 48 h, and all volatiles were removed under reduced pressure. Toluene (30 mL) was added to the residue, and insoluble substances were removed by filtration. The solution was reduced in volume to 5 mL and stored at –30 °C to obtain **17** as a white solid. Yield: 1.71 g (70%). $C_{14}H_{13}BrF_5N_2Sb$ (505.92): calcd. C 33.24, H 2.59, N 5.54; found C 33.05, H 2.51, N 5.33. EI-MS: *m*/*z* (%) = 506 (2) [M]$^+$, 247 (100) [M – N(C_5H_4N)(C_6F_5)]$^+$. ^1H NMR (C_6D_6, 200.13 MHz): δ = 1.79 (s, 9 H, $SbMe_3$), 5.55–5.59 (m, 1 H), 6.20–6.27 (m, 1 H), 6.85–6.94 (m, 1 H), 7.58–7.61 (m, 1 H) ppm. ^{13}C NMR (C_6D_6, 50.32 MHz): δ = 20.83 ($SbMe_3$), 106.31, 113.53, 138.57, 146.21, 159.07 ppm; 4 signals for the carbon atoms of the C_6F_5 group were not observed in the spectrum. ^{19}F NMR (C_6D_6, 188.28 MHz): δ = –162.18 (t, 2 F), –157.64 (t, 1 F), –147.22 (d, 2 F) ppm.

Synthesis of 18: The procedure was analogous to that used to synthesize **17**. Thus, treatment of a solution of **4**·thf (1.10 g, 3.24 mmol) in thf (20 mL) with a solution of **8** (0.77 g, 3.24 mmol) in thf (15 mL) gave **18** as a white solid. Yield: 1.15 g (77%). $C_{14}H_{13}ClF_5N_2Sb$ (461.47): calcd. C 36.44, H 2.84, N 6.07; found C 36.21, H 2.71, N 5.72. FD-MS: *m*/*z* (%) = 462 (1) [M]$^+$, 384 (100) [M – C_5H_4N]$^+$. ^1H NMR (C_6D_6, 200.13 MHz): δ = 1.67 (s, $SbMe_3$), 5.56–5.61 (m, 1 H), 6.21–6.28 (m, 1 H), 6.86–6.95 (m, 1 H), 7.63–7.64 (m, 1 H) ppm. ^{13}C NMR (C_6D_6, 50.32 MHz): δ = 19.95 ($SbMe_3$), 106.80, 113.63, 138.58, 146.43, 158.78 ppm; 4 signals for the carbon atoms of the C_6F_5 group were not observed in the spectrum. ^{19}F NMR (C_6D_6, 188.28 MHz): δ = –162.31 (t, 2 F), –158.10 (t, 1 F), –147.31 (d, 2 F) ppm.

Synthesis of 19: The procedure was analogous to that used to synthesize **17**. Thus, treatment of a solution of **4**·thf (2.64 g, 7.80 mmol) in thf (20 mL) with a solution of **8** (0.93 g, 3.90 mmol) in thf (15 mL) gave **19** as a white solid (extraction with *n*-pentane). Yield: 1.95 g (73%). $C_{25}H_{17}F_{10}N_4Sb$ (685.17): calcd. C 43.82, H 2.50, N 8.18; found C 43.58, H 2.35, N 7.66. EI-MS: *m*/*z* (%) = 669 (1) [M – Me]$^+$, 425 (100) [M – N(C_5H_4N)(C_6F_5)]$^+$. ^1H NMR (C_6D_6, 200.13 MHz): δ = 1.29 (br. s, $SbMe_3$), 5.96–6.00 (m, 2 H), 6.31–6.37 (m, 2 H), 6.94–7.02 (m, 2 H), 8.04–8.06 (m, 2 H) ppm. ^{13}C NMR (C_6D_6, 50.32 MHz): δ = 19.76 ($SbMe_3$), 106.80, 112.48, 138.49, 146.29, 159.51 ppm; 4 signals for the carbon atoms of the C_6F_5 group were not observed in the spectrum. ^{19}F NMR (C_6D_6, 188.28 MHz): δ = –164.27 (t, 4 F), –161.72 (t, 2 F), –146.97 (d, 4 F) ppm.

X-ray Crystallographic Study. Crystal Data for 9·0.5C_7H_8: Triclinic unit cell, space group $P\bar{1}$, with a = 10.7275(8), b = 12.9882(8), c = 14.4190(10) Å, α = 72.264(8), β = 79.030(9), γ = 69.388(8)°, V = 1783.2(2) Å^3, Z = 2. 17664 reflections were collected at 193 K with a STOE IPDS diffractometer using graphite-monochromated Mo-K_α radiation and were corrected for absorption. 6471 reflections were unique (R_{int} = 0.0517) and 4274 with $I > 2\sigma(I)$ "observed". The structure was solved by direct methods[33] and refined using the full-matrix least-squares procedure.[34] All non-hydrogen atoms were treated anisotropically, and hydrogen atoms were treated with fixed isotropic thermal parameters as "riding" on calculated positions. One molecule of disordered toluene is present in the unit cell and was refined with restraints for geometrical and thermal parameters. Final residuals for 540 refined parameters and 70 restraints: $wR2$ = 0.053 (for all unique data), $R1$ = 0.0314 (for the "observed" data). CCDC-631484 (**9**) contains the supplementary crystallographic data for this paper. These data can be obtained free of charge from The Cambridge Crystallographic Data Centre via www.ccdc.cam.ac.uk/data_request/cif.

Supporting Information (see footnote on the first page of this article): Molecular structures of stable compounds and transition states with and without $M \rightarrow N_{Py}$ intramolecular interactions [series (a) and (b)], their calculated Cartesian coordinates, energies, and numbers of imaginary frequencies.

Acknowledgments

We thank Dr. D. N. Laikov for providing us with the program PRIRODA. We also thank the Research Computing Center of the Moscow State University for computational time.

[1] P. L. Shutov, S. S. Karlov, K. Harms, D. A. Tyurin, J. Sundermeyer, J. Lorberth, G. S. Zaitseva, *Eur. J. Inorg. Chem.* **2004**, 2498–2503.
[2] *Organofluorine Chemistry: Principles and Commercial Applications* (Eds.: R. E. Banks, B. E. Smart, J. C. Tatlow), Plenum, New York, **1994**.
[3] T. Hiyama, *Organofluorine Compounds*, Springer, Berlin, **2000**.
[4] U. Mazurek, H. Schwarz, *Chem. Commun.* **2003**, 1321–1326.
[5] J. L. Kiplinger, T. G. Richmond, C. E. Osterberg, *Chem. Rev.* **1994**, *94*, 373–431.
[6] T. Braun, S. P. Foxon, R. N. Perutz, P. H. Walton, *Angew. Chem. Int. Ed.* **1999**, *38*, 3326–3329.
[7] T. G. Richmond, C. E. Osterberg, A. M. Arif, *J. Am. Chem. Soc.* **1987**, *109*, 8091–8092.
[8] T. Schaub, M. Backes, U. Radius, *J. Am. Chem. Soc.* **2006**, *128*, 15964–15965.
[9] S. Park, M. Pontier-Johnson, D. M. Roundhill, *J. Am. Chem. Soc.* **1989**, *111*, 3101–3103.
[10] L. Maron, E. L. Werkema, L. Perrin, O. Eisenstein, R. A. Andersen, *J. Am. Chem. Soc.* **2005**, *127*, 279–292.
[11] U. Jäger-Fiedler, P. Arndt, W. Baumann, A. Spannenberg, V. V. Burlakov, U. Rosenthal, *Eur. J. Inorg. Chem.* **2005**, 2842–2849.
[12] J. Burdeniuc, B. Jedlicka, R. H. Crabtree, *Chem. Ber./Recueil* **1997**, *130*, 145–154.
[13] G. M. Brooke, *J. Fluorine Chem.* **1997**, *86*, 1–76.
[14] T. N. Gerasimova, N. A. Orlova, *J. Fluorine Chem.* **1985**, *28*, 361–380.
[15] F. V. Cochran, P. J. Bonitatebus, R. R. Schrock, *Organometallics* **2000**, *19*, 2414–2416.
[16] A. N. Frolov, *Russ. J. Org. Chem.* **1998**, *34*, 1047–1051.
[17] R. Koppang, *J. Organomet. Chem.* **1972**, *46*, 193–200.
[18] J. Ashenhurst, L. Brancaleon, S. Gao, W. Liu, H. Schmider, S. Wang, G. Wu, Q. G. Wu, *Organometallics* **1998**, *17*, 5334–5341.
[19] F. H. Allen, *Acta Crystallogr., Sect. B* **2002**, *58*, 380–388.
[20] R. A. Fischer, H. Sussek, A. Miehr, H. Pritzkow, E. Herdtweck, *J. Organomet. Chem.* **1997**, *548*, 73–80.
[21] J. Emsley, *The Elements*, 3rd ed., Clarendon Press, Oxford, U.K., **1998**.
[22] P. L. Shutov, S. S. Karlov, K. Harms, D. A. Tyurin, A. V. Churakov, J. Lorberth, G. S. Zaitseva, *Inorg. Chem.* **2002**, *41*, 6147–6152.
[23] M. Jakt, L. Johannissen, H. S. Rzepa, D. A. Widdowson, R. Wilhelm, *J. Chem. Soc. Perkin Trans. 2* **2002**, 576–581.
[24] T. Braun, R. N. Perutz, *Chem. Commun.* **2002**, 2749–2757.
[25] W. D. Jones, *Dalton Trans.* **2003**, 3991–3995.
[26] W. Clegg, N. A. Compton, R. J. Errington, G. A. Fisher, M. E. Green, D. C. R. Hockless, N. C. Norman, *Inorg. Chem.* **1991**, *30*, 4680–4682.
[27] G. Rosetto, N. Brianese, A. Camporese, M. Porchia, P. Zanella, R. Bertoncello, *Main Group Met. Chem.* **1991**, *14*, 113–122.
[28] B. A. Nevett, A. Perry, *Spectrochim. Acta* **1975**, *A31*, 101–107.
[29] T. Okada, R. Okarawa, *J. Organomet. Chem.* **1973**, *54*, 149–152.
[30] J. P. Perdew, K. Burke, M. Ernzerhof, *Phys. Rev. Lett.* **1996**, *77*, 3865–3868.
[31] M. Ernzerhof, G. E. Scuseria, *J. Chem. Phys.* **1999**, *110*, 5029–5036.
[32] D. N. Laikov, *Chem. Phys. Lett.* **1997**, *281*, 151–156.
[33] *SIR92 – A program for crystal structure solution*: A. Altomare, G. Cascarano, C. Giacovazzo, A. Guagliardi, *J. Appl. Crystallogr.* **1993**, *26*, 343–350.
[34] G. M. Sheldrick, *SHELXL97 – Program for Crystal Structure Refinement*, release 97-2, University of Göttingen, Germany, **1997**.

Received: July 22, 2007
Published Online: November 8, 2007

